Elastic Properties of Microcomponents under Uniaxial Stress

K. Jöchen[*] and **T. Böhlke**[**]

Lehrstuhl für Kontinuumsmechanik, Institut für Technische Mechanik, Universität Karlsruhe (TH), Postfach 6980, 76128 Karlsruhe, Germany

In order to develop highly stressable microcomponents for various applications, the structural behavior of such parts has to be examined with respect to an accurate prediction of the elastic and plastic characteristics. When simulating microparts, the major challenge is to capture the significant material heterogeneities, which are the result of the small geometrical dimensions of the components being of the same order of magnitude as the grain size. For this reason, the concept of effective properties fails and apparent properties have to be considered. In this paper we examine the elastic properties of microspecimens made of gold. Therefore, various finite element simulations have been evaluated statistically in order to identify the characteristic parameters of the distribution. Polycrystals are modeled as a periodic Voronoi tesselation with a uniform distribution of crystal orientations.

1 Elastic properties of gold

1.1 Single crystals

Gold has a cubic crystal symmetry, therefore, three independent elastic constants describe the elastic material behavior of the single crystal. Using the projector representation of the elasticity tensors, we can write [1]

$$\mathbb{C} = \sum_{i=1}^{3} \lambda_i \mathbb{P}_i, \qquad \mathbb{S} = \sum_{i=1}^{3} \frac{1}{\lambda_i} \mathbb{P}_i \tag{1}$$

with the eigenvalues $\lambda_1 = C_{1111} + 2C_{1122}$, $\lambda_2 = C_{1111} - C_{1122}$ and $\lambda_3 = 2C_{2323}$ and the cubic projectors $\mathbb{P}_1 = 1/3\, \boldsymbol{I} \otimes \boldsymbol{I}$, $\mathbb{P}_2 = \mathbb{D} - \mathbb{P}_1$, $\mathbb{P}_3 = \mathbb{I}^S - \mathbb{D}$. The anisotropic part $\mathbb{D}$ of the projectors contains the lattice vectors $\boldsymbol{g}_i$

$$\mathbb{D} = \sum_{i=1}^{3} \boldsymbol{g}_i \otimes \boldsymbol{g}_i \otimes \boldsymbol{g}_i \otimes \boldsymbol{g}_i. \tag{2}$$

Young's modulus of a single crystal can be calculated subject to an arbitrary loading direction $\boldsymbol{d}$ [2]

$$\frac{1}{E(\boldsymbol{d})} = \boldsymbol{d} \otimes \boldsymbol{d} \cdot \mathbb{S}[\boldsymbol{d} \otimes \boldsymbol{d}] \tag{3}$$

with the compliance tensor $\mathbb{S} = \mathbb{C}^{-1}$. $E(\boldsymbol{d})$ is bounded by its extremal values, located at the $\langle 100 \rangle$ and $\langle 111 \rangle$ crystal direction.

1.2 Polycrystals

The orientation of each single crystal is described by a proper orthogonal tensor $\boldsymbol{Q} \in SO(3)$ which maps a fixed reference basis $\boldsymbol{e}_i$ onto the lattice vectors $\boldsymbol{g}_i = \boldsymbol{Q}\boldsymbol{e}_i$. For modeling a polycrystalline sample, we assume that every orientation is equiprobable. If the number of grains in the sample tends to infinity (isotropic material), the shear modulus is bounded by the well-known isotropic Voigt and Reuss bounds [3, 4]

$$2G^V = \bar{\lambda}_2^V = \frac{2}{5}\lambda_2 + \frac{3}{5}\lambda_3, \qquad (2G^R)^{-1} = (\bar{\lambda}_2^R)^{-1} = \frac{2}{5}\lambda_2^{-1} + \frac{3}{5}\lambda_3^{-1}. \tag{4}$$

A closer estimation of the upper and the lower bound for the shear modulus can be obtained by the Hashin-Shtrikman bounds [5]

$$\begin{aligned} 2G^{HS-} &= \bar{\lambda}_2^{HS-} = \lambda_2 + 3\left(\frac{5}{\lambda_3 - \lambda_2} + 4\frac{\lambda_1 + 3\lambda_2}{5\lambda_2(\lambda_1 + 2\lambda_2)}\right)^{-1}, \\ 2G^{HS+} &= \bar{\lambda}_2^{HS+} = \lambda_3 + 2\left(\frac{5}{\lambda_2 - \lambda_3} + 6\frac{\lambda_1 + 3\lambda_3}{5\lambda_3(\lambda_1 + 2\lambda_3)}\right)^{-1}. \end{aligned} \tag{5}$$

The first isotropic eigenvalue, which is thrice the bulk modulus, is identical to the first cubic one $3K = \bar{\lambda}_1^R = \bar{\lambda}_1^V = \bar{\lambda}_1^{HS} = \lambda_1$. Young's modulus of an isotropic estimate can be determined by $\bar{E} = (3\bar{\lambda}_1\bar{\lambda}_2)/(2\bar{\lambda}_1 + \bar{\lambda}_2)$.

[*] Corresponding author E-mail: joechen@itm.uni-karlsruhe.de, Phone: +49 721 608 6900
[**] boehlke@itm.uni-karlsruhe.de

2 FE based homogenization of elastic properties

The experimental stress-strain curves for specimens made of Stabilor®G, which is primarily composed of gold and, therefore, shows a similar mechanical behavior, can be seen in Fig. 1 (left) [6,7]. In the elastic as well as in the plastic region, a scattering of the slope of the curves, denoting Young's modulus and the hardening behavior, can be identified. Furthermore, there exists a broad variation of the initial yield stress.

The FE program ABAQUS has been used to carry out simulations of uniaxial tensile tests. Discretizing the tensile specimen, 45000 hexahedral elements are taken in order to reproduce a variety of numbers of grains in the sample volume with the same model. In the FE model, the microstructure is represented as a periodic Voronoi tessellation. In order to determine mean values and standard deviations of Young's modulus, 300 different discrete orientation distributions have been examined for each of the number of grains considered in this study.

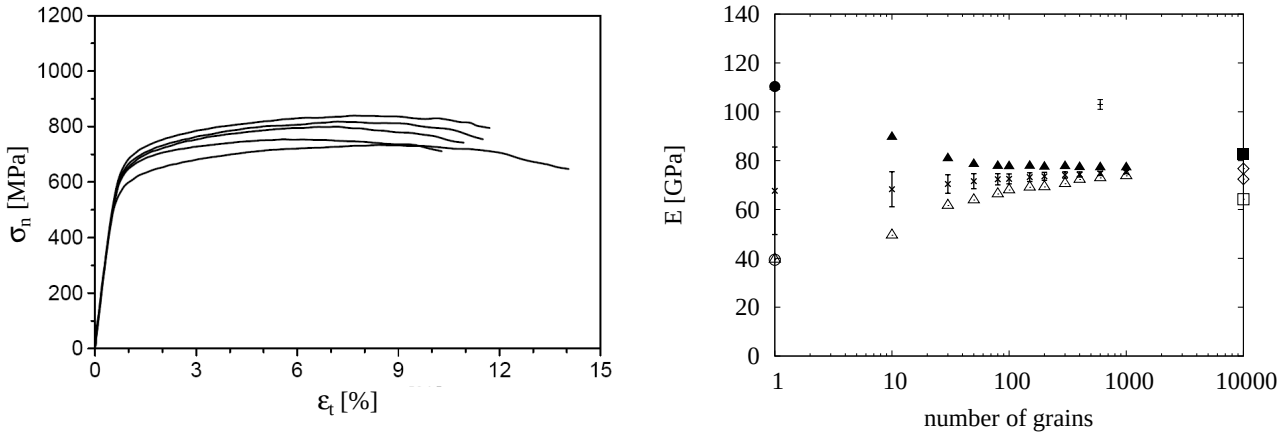

Fig. 1 Left: experimental stress-strain curves [7]; Right: Young's modulus of gold for different numbers of grains in the sample: ■ Voigt upper bound, □ Reuss lower bound, ◇ Hashin-Shtrikman bounds, × arithmetic mean of Young's modulus from simulations, ▲ maximum Young's modulus in simulations, △ minimum Young's modulus in simulations, ● Young's modulus in $\langle 111 \rangle$-direction, ○ Young's modulus in $\langle 100 \rangle$-direction, + experimental results

The scattering of Young's modulus of gold for different numbers of grains in the specimen is shown in Fig. 1 (right). The arithmetic mean and the standard deviation are denoted with errorbars in between the extremal values of the simulations. With an increasing number of grains the macroscopic material behavior gets less anisotropic, which is indicated by a decreasing scattering of Young's modulus. Moreover, the arithmetic mean tends between the Hashin-Shtrikman bounds. So, this estimation, which is much more narrow than the Voigt and Reuss bounds, agrees well with the results obtained by simulations for weakening anisotropy in the specimen.

The errorbar with the plus sign located at 600 grains shows experimental data of tensile tests of the alloy Stabilor®G. The experimentally determined Young's modulus ($E_{600}^{\mathrm{exp}} = 103 \pm 2$ GPa) differs significantly from the one identified by the simulations for pure gold ($E_{600}^{\mathrm{num}} = 74.7 \pm 0.8$ GPa).

3 Conclusion

In this work, simulations have been carried out in order to examine the variation of Young's modulus of polycrystalline specimens for different numbers of grains. Compared to experiments for Stabilor®G, Young's modulus having been numerically determined by the usage of the elastic constants of gold is too low. Therefore, we propose a uniform scaling of the underlying eigenvalues λ_i with an approximate factor of 1.4 in order to capture the experiments. The magnitude of the scattering of Young's modulus obtained by the simulations agrees with the experimental findings.

References

[1] P. Halmos, Finite-Dimensional Vector Spaces (D. van Nostrand Company, Inc., New York, 1958).
[2] T. Böhlke and C. Brüggemann, Technische Mechanik **21**(2), 145–158 (2001).
[3] W. Voigt, Lehrbuch der Kristallphysik (Teubner Leipzig, 1910).
[4] A. Reuss, Z. Angew. Math. Mech. **9**, 49–58 (1929).
[5] Z. Hashin and S. Shtrikman, J. Mech. Phys. Solids **10**, 343–352 (1962).
[6] M. Auhorn, B. Kasanická, T. Beck, V. Schulze, and D. Löhe, Microsystems Technologies **12**, 713–716 (2006).
[7] M. Auhorn, Mechanische Eigenschaften urgeformter Mikroproben aus Au58Ag23Cu12Pd5 und ZrO_2, PhD thesis, Universität Karlsruhe (TH), 2005.